DOI: 10.61782/fa.2023.1091

forum acusticum 2023

BEAMFORMING ALGORITHM FOR VEHICLE CABIN ACOUSTIC COMFORT APPLICATION

Francesco Uffreduzzi[1*] **Alessandro Aquili**[1] **Elisa de Paola**[2]
Luana G. Stoica[2] **Alessandro Di Marco**[2]
[1] Pininfarina S.p.A., Torino, Italy
[2] Department of Civil, Computer Science and Aeronautical Technologies Engineering, University of Roma Tre, Roma, Italy

ABSTRACT

The growing importance of electric vehicles in the global market makes the reduction of wind noise a crucial point to invest money and resources on. To improve the car acoustic comfort, it is now more than before necessary to identify properly the aeroacoustic sound sources around the vehicle, which were previously masked by the engine noise. The beamforming techniques are widely used methods which, based on one or more arrays of microphones, are able to localize the noise sources on a virtual plane close to the object. Not all the sources highlighted, however, are able to reach the car cabin and affect its acoustic comfort. Based on these considerations, Pininfarina Wind Tunnel and Roma Tre University started a research program to understand which of the various sound sources detected by the beamforming algorithm shows a correlation with a simultaneously measured reference signal, placed inside the car at the driver and passengers head position. This approach aims at providing more effective tools to the vehicle manufacturers able to help them in the development of even more performing and comfortable vehicles.

Keywords: *wind tunnel, beamforming, car noise, aeroacoustic, acoustic comfort*

**Corresponding author*: *F.Uffreduzzi@pininfarina.it.*

1. INTRODUCTION

The automotive industry has largely benefited from the improvements in microphone array techniques over the last two decades. The most common wind tunnel application for wind noise investigation is the use of out-of-flow planar beamforming arrays to localize and quantify exterior aeroacoustic noise sources such as side-view mirror, A-pillar, wheelhouse arch etc. Through continuous developments, the sound maps of today are significantly more detailed compared to the past. Nevertheless, classical beamforming formulations cannot evaluate the real impact of exterior noise sources on interior noise level.

Beamforming using a spherical array of microphones installed inside the car cabin allows for the identification of the areas which contribute most to the interior noise level. However, this characterization is not sufficient to accurately localize the exterior aeroacoustic sources responsible for these emissions.

The purpose of the present work is therefore to develop an algorithm capable of evaluating the contribution of external sources to interior noise level by correlating the arrays signals with an additional microphone installed inside the vehicle.

2. PININFARINA WIND TUNNEL FACILITY

To investigate the external noise sources of vehicles in the full scale wind tunnel, Pininfarina uses, since 2005, a beamforming system based on microphones arrays. This system allows to identify the noise sources in a virtual plane close to the vehicle and parallel to the one in which the microphones lie. The wind tunnel is equipped with:

- an overhead array, located on the ceiling of the test section (4m from the floor) which consists of 78 microphones (Figure 1)
- a lateral array, placed on the side wall of the test section with 66 microphones (Figure 1)
- a smaller frontal array, installed above the nozzle exit, with 15 microphones (Figure 2)

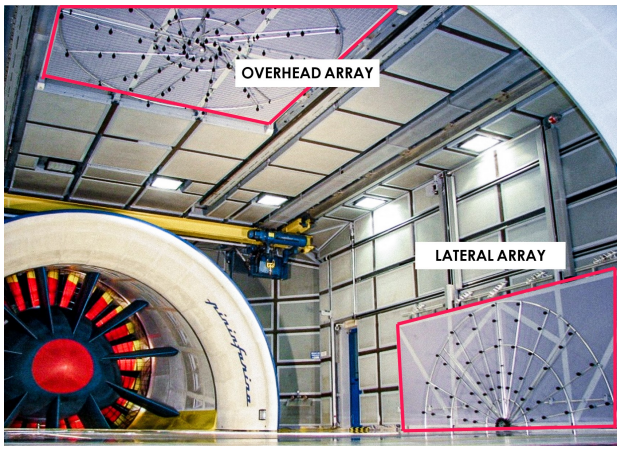

Figure 1. Pininfarina side and overhead arrays

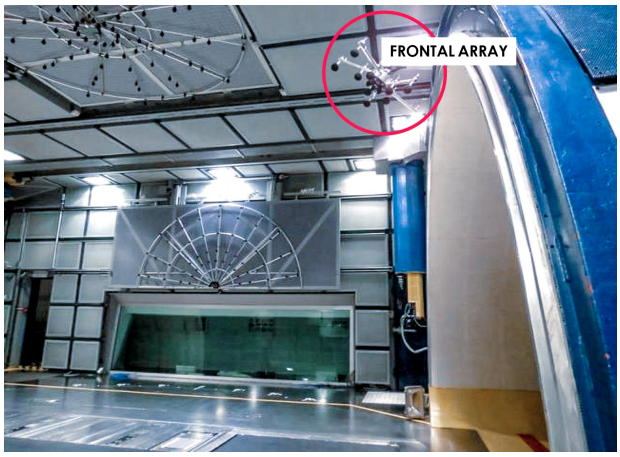

Figure 2. Pininfarina frontal array

3. ALGORITHM

The Pininfarina conventional beamforming algorithm is based on the cross-spectral imaging function, deeply described in [1]. The coherence beamforming technique introduced here takes inspiration from [2] and makes use of an additional reference microphone recorded synchronously with the external arrays. The coherent beamformer power output requires the computation of a cross-spectral matrix defined, for a single frequency and a single microphone, as follows:

$$C_{xy}(i_{Mik}, f) = \frac{1}{N_w} \sum_{k=1}^{N_w} P_{i_{Mik}}(f) P_{Ref}(f)^* \quad (1)$$

where $P_{i_{Mik}}$ is the two-sided FFT of the i^{th} microphone, P_{Ref} is the two-sided FFT of the reference microphone and the symbol $(.)^*$ stands for the complex-conjugate operator. The single-sided form of the cross spectral matrix is then obtained by multiplying each frequency by two and discarding the second half of the array.

This formulation leads to an output influenced by the arrays signals and tends to amplify the coherent beamformer power output compared to the levels measured inside the cabin, when there is a high coherence between the internal recorded signal and the external ones. To avoid this, the cross spectral matrix has been rescaled as follows:

$$\overline{C_{xy}(i_{Mik}, f)} = \frac{1}{N_w} \sum_{k=1}^{N_w} 2 \cdot \frac{P_{i_{Mik}}(f) P_{Ref}(f)^*}{\sqrt{P_{i_{Mik} i_{Mik}}(f)}} \quad (2)$$

where $P_{i_{Mik} i_{Mik}}(f)$ is the i^{th} microphone average power spectrum computed as:

$$P_{i_{Mik} i_{Mik}}(f) = \frac{1}{N_w} \sum_{k=1}^{N_w} P_{i_{Mik}}(f) P_{i_{Mik}}(f)^* \quad (3)$$

The coherent beamformer power output, for a single grid point x_G and a single frequency f, is then obtain from:

$$P_{Coh}(x_G, f) = \frac{1}{N_{Miks}} \sum_{i_{Mik}=1}^{N_{Miks}} \overline{C_{xy}(i_{Mik}, f)} e^{j2\pi f \frac{d_{i_{Mik}}}{c}} \quad (4)$$

where $d_{i_{Mik}}$ is the distance of the i^{th} microphone from the grid point x_G and c is the speed of sound.

4. VALIDATION TEST CASE

4.1 Experimental set-up

For the validation test case, a Brüel and Kjær Omnisource Sound Source Type 4295 has been chosen. The size of the orifice and the shape have been carefully engineered to radiate sound evenly in all directions. Thus, Type 4295 fulfils the national and international standards for omnidirectional sound sources, as reported in Figures 3 and 4.

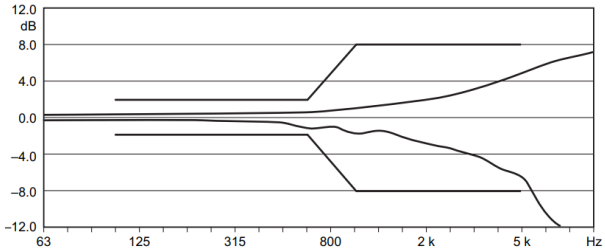

Figure 3. Maximum allowed directional deviation of an omnidirectional sound source according to ISO 140 (averaged over 'gliding' 30° arcs in a free sound field). Upper and lower curves are the ISO tolerances

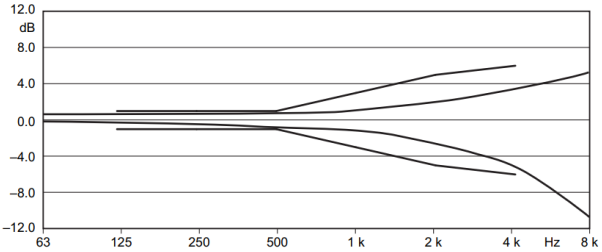

Figure 4. Maximum allowed directional deviation of an omnidirectional sound source according to ISO 3382-1 (averaged over 'gliding' 30° arcs in a free sound field). Upper and lower curves are the ISO tolerances

The experimental set-up arranged for the validation test case is shown in Figure 5. The Brüel and Kjær Omnisource Sound Source Type 4295 has been placed 3m from the side array center and 2.8m from the overhead array in order to replicate real automotive test conditions (in terms of distances between the source and the arrays).

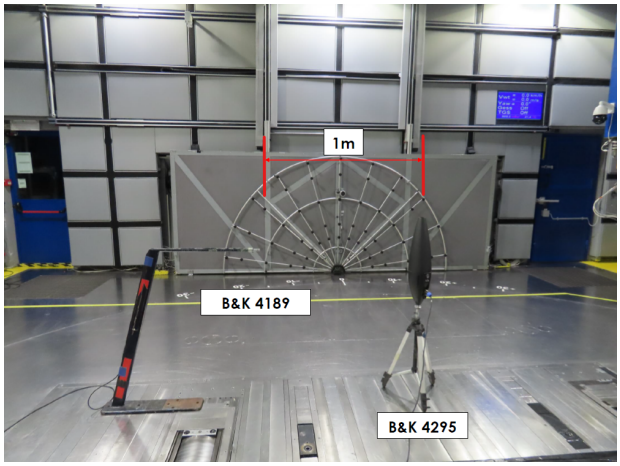

Figure 5. Validation test case experimental set-up

A Brüel and Kjær 4189 free field reference microphone has been positioned at 1m from the source. The microphone has the specifications reported in Table 1 and its typical free field response is depicted in Figure 6.

Table 1. Brüel and Kjær 4189 specifications

Sensitivity	50 mV/Pa
Frequency	6.3 Hz - 20 kHz
Dynamic Range	14.6 - 146 dB
Temperature	-30 to +150 °C
Polarization	prepolarized

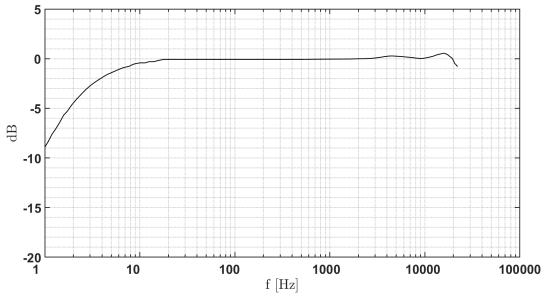

Figure 6. Typical free-field response of Brüel and Kjær 4189 microphone with protection grid

4.2 Results

In order to validate the algorithm, a white noise signal has been used. The reference microphone has been synchronously acquired along with the arrays receivers, considering an acquisition time $T = 6.25$ s and a sampling frequency $f_s = 32768$ Hz. The frequency range of interest spans from 250 to 5000 Hz. Only the results obtained from the overhead array will be discussed in this paper.

Figure 7 shows a comparison between the source Sound Pressure Level (SPL) measured by the reference microphone and the one obtained through the conventional and coherence beamforming algorithm. All the array spectra are calculated at 1m from the source. The curves retrieved by the two beamforming algorithms are plotted considering the maximum SPL value obtained on the zone of interest for each frequency.

As it can be observed, all the curves are in good agreement over the whole frequency range, and the coherence beamforming algorithm results follow the reference microphone SPL very well.

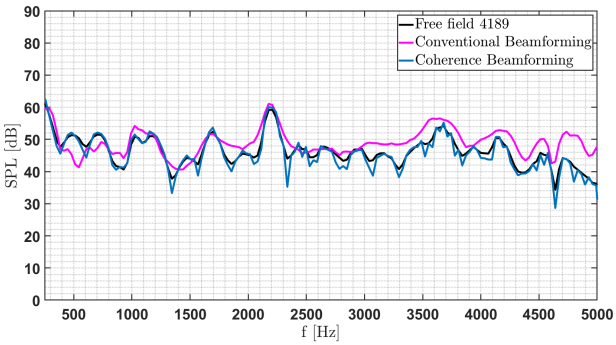

Figure 7. SPL at 1m from the source - conventional and coherence beamforming algorithm vs reference microphone

Focusing on the sound maps, the coherence beamforming algorithm results match the conventional methodology in terms of source localization, providing slightly different SPL values since the signal is statistically conditioned by the correlation with the reference microphone. An example of sound maps for the one-third octave band centered at 2500 Hz is reported in Figure 8.

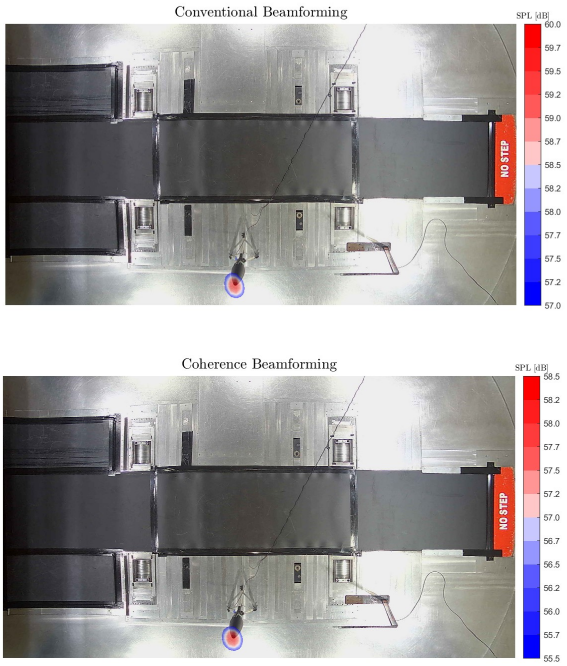

Figure 8. Example of sound maps in one-third octave bands - f=2500 Hz - conventional vs coherence beamforming

5. REAL CASE

5.1 Experimental set-up

For the real case, all the measurements have been performed on a production car. A Brüel and Kjær diffuse field 4942 microphone has been positioned inside the car, at the driver head position, oriented towards the side-view mirror (see Figure 9). In addition a KingState KPE-141 source has been installed as highlighted in Figure 10. The tonal noise frequency emitted by this source has been set to 3850 Hz.

Figure 9. Diffuse field microphone installation inside the car

Figure 10. KingState KPE-141 noise generator installation on the car

The microphone has the specifications reported in Table 2 and its typical random-incidence response is depicted in Figure 11.

Table 2. Brüel and Kjær 4942 specifications

Sensitivity	50 mV/Pa
Frequency	6.3 Hz - 16 kHz
Dynamic Range	14.6 - 146 dB
Temperature	-40 to +150 °C
Polarization	0 V

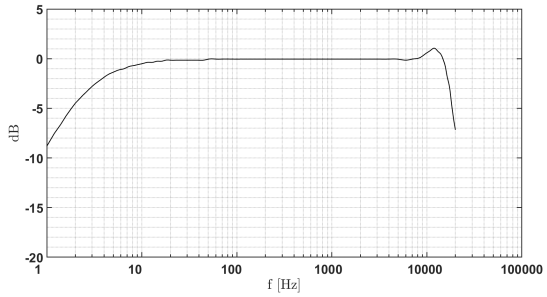

Figure 11. Typical random-incidence response of a Brüel and Kjær 4942 microphone with protection grid

Tests have been performed at various wind tunnel flow speeds. In the following paragraphs the most important results obtained from this investigation will be highlighted. The frequency range of interest has been focused between 250 and 6000 Hz.

5.2 Results

5.2.1 V = 60 kph - KingState source ON

Figure 12 shows a comparison between the SPL measured by the reference microphone and the one obtained through the conventional and coherence beamforming algorithm. In the latter case, a peak is found whenever there is a high level of coherence between the external receivers and the internal one. This means that what is measured by the external array is able to pass inside the car cabin and is also perceived inside the vehicle.

For the real case presented, the array spectra have been calculated at the array plane.

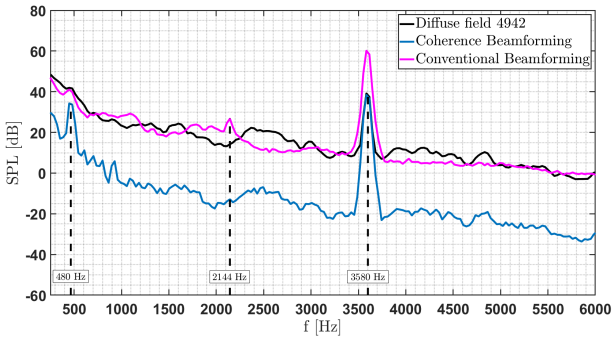

Figure 12. SPL at V=60kph - conventional and coherence beamforming algorithm vs reference microphone

The peak occurring at $f = 480$ Hz is due to a noise generator located in the rear part of the vehicle, as depicted in Figure 13.

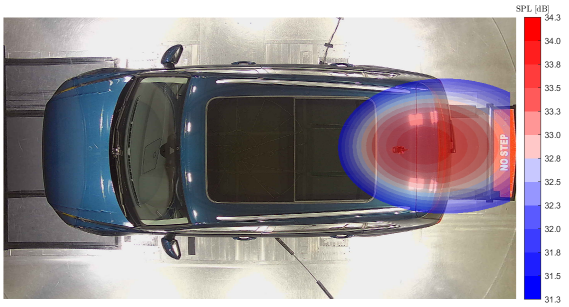

Figure 13. Sound map in one-third octave bands - f=500 Hz - coherence beamforming

At first glance, it could be attributed to the main fan, which is few meters behind the car. However, the following investigations proved that it came from the trunk:

- A subjective evaluation was used to localize the low frequency noise in the trunk area
- A parametric investigation, moving the car forward by 400mm, resulted in a source shift which followed the vehicle displacement (see Figure 14)

The coherence beamforming algorithm, combining the information coming from the external and internal measurements, allowed to highlight a noise source which was not so evident by looking only at the conventional beamforming and the reference microphone spectra. In both cases, only a slight peak could be noticed, masked by the background noise.

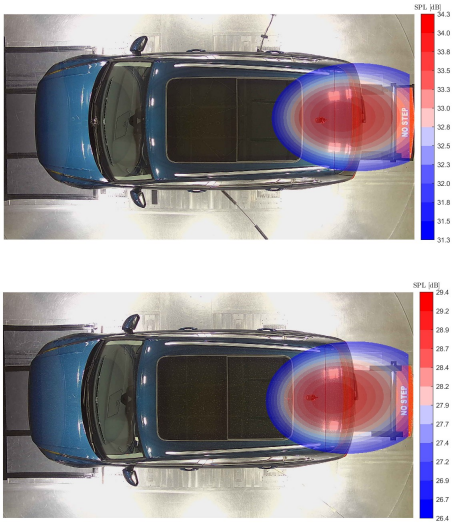

Figure 14. Sound map in one-third octave bands - f=500 Hz - coherence beamforming - Nominal position (on top) vs car shifted forward (on bottom)

A second peak can be seen at f=2144 Hz, but only in conventional beamforming integrated spectra and not in the coherence beamforming one. This tonal emission is produced by the vehicle front grille and is therefore perceived only from outside. Figure 15 shows a comparison between the sound maps obtained using the two algorithms in the frequency range 2050-2250 Hz. While the conventional beamforming precisely localizes the noise source, the coherence beamforming fails due to a low level of correlation between the external receivers and the internal reference one. This is also evident by looking at the very low SPL values obtained from the map.

The tonal noise emitted by the synthetic source is well detected by the microphone array, as depicted in Figure 16, and is also perceived by the internal microphone. Both sound levels show good agreement.

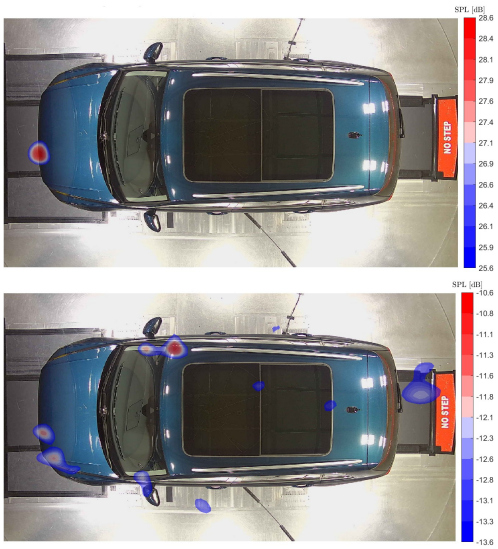

Figure 15. Sound map in the frequency range 2050-2250 Hz - conventional beamforming (on top) vs coherence beamforming (on bottom)

Figure 16. Sound map in one-third octave bands - f=4000 Hz - coherence beamforming

5.2.2 V = 100 kph - KingState source ON

As the wind tunnel flow speed is increased, a new peak can be found in the coherence beamforming SPL integrated spectrum, as shown in Figure 17. The vehicle front grille produces a tonal noise at $f = 2368$ Hz which is heard both from outside and inside the car cabin and can be seen in the third-octave sound map shown in Figure 18.

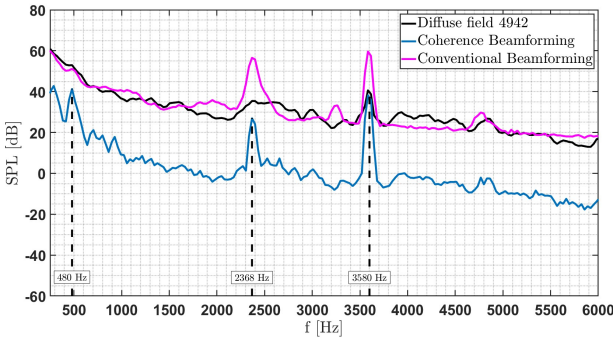

Figure 17. SPL at V=100kph - conventional and coherence beamforming algorithm vs reference microphone

Figure 18. Sound map in one-third octave bands - f=2500 Hz - coherence beamforming

The coherence beamforming spectrum also reveals three lower peaks in the 600 and 1000 Hz frequency range that can be ascribed to the flow interaction with the left side-view mirror. Performing the coherence between the signals acquired by the array and the internal microphone, only the noise emitted by this sound source shows high levels of correlation.

Figure 19 shows a comparison, for three different one-third octave bands, between the sound maps obtained through the conventional beamforming algorithm and the maps obtained through the coherence beamforming. As can be seen, the conventional beamforming tends to adequately localize the noise sources around the windshield and the front of the car, while the coherence beamforming precisely localizes the origin of the noise on the left side-view mirror.

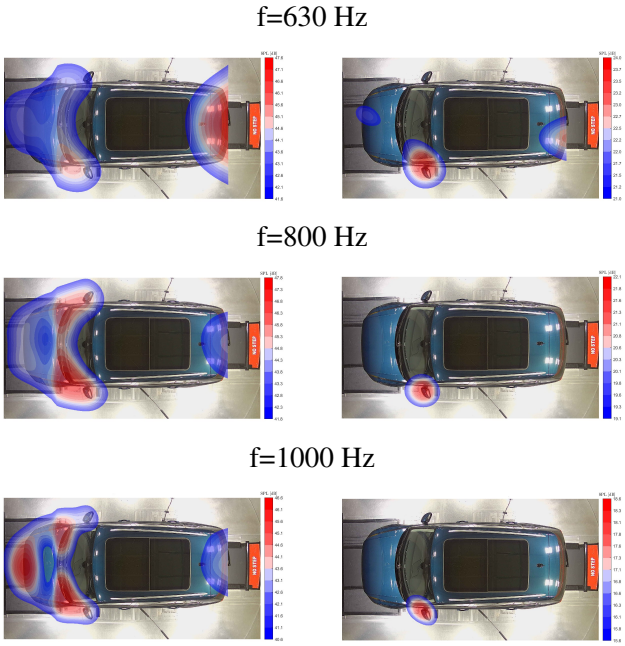

Figure 19. Conventional beamforming (on the right) vs coherence beamforming (on the left) for three different one-third octave bands

6. CONCLUSIONS

This work proposes the implementation and application of coherence based beamforming in the frame of an automotive aeroacoustic wind tunnel testing. The method is first assessed with a known source of noise and then tested on a real case, comparing the results with a conventional beamforming algorithm. conventional beamforming clearly identifies the location of major sound sources but fails if low intensity sound sources are masked by louder ones or by broadband frequency noise. The method utilized takes a reference signal so as to denoise the microphones arrays. This removes the aerodynamic noise contribution in order to individuate the impact of outside sources on the interior noise. Results of the coherence based beamforming successfully evidence the major noise sources responsible for passengers discomfort, otherwise unrecognized with conventional approaches. This helps to enhance the aerodynamic noise measurement in the automotive industry, allowing for improved evaluation of passenger comfort.

7. REFERENCES

[1] J. Christensen and J. Hald, "Beamforming," *Brüel and Kjær Technical Review*, no. 1, 2004.

[2] M. Garcia-Pedroche and G. J. Bennett, "Aeroacoustic Noise Source Identification Using Irregularly Sampled LDV Measurements Coupled with Beamforming.," *AIAA/CEAS Aeroacoustics Conference*, 6 2011.